OPTIMUM DESIGN OF FUNCTIONALLY GRADED PLATES UNDER THERMAL SHOCK

Farid Vakili-TAHAMI[1], Nima MAHKAM[2], Arash Mohammad Alizadeh FARD[3]

Optimum design of a Functionally Graded plate, which is suddenly exposed to a temperature gradient, is studied in this paper. A unique method is developed based on the combination of both discretization and Fourier series to obtain the time-dependent temperature and thermal stresses on the plate, by taking into account the material distribution. The effect of Graded Material is implemented using Mori-Tanaka method along with Fuzzy logic. Two optimization methods, Genetic algorithm and Particle Swarm Optimization, has been used to calculate the optimum values of volume fraction distribution to provide optimum strength ratio along z direction of the plate.

Keywords: Functionally Graded Materials, Thermal Shock, Plate, Optimum Mechanical Design

1. Introduction

Functionally graded materials (FGMs) are a new class of composite materials wherein the composition of each material constituent varies gradually with respect to spatial coordinates. Each varying composition is designed to take advantage of its attractive features. For example, for advanced high temperature structural applications a type of materials is required to have strength at high temperature, creep resistance, adequate toughness and thermal shock resistance. Ceramics possess low density, good high temperature strength and creep resistance, whereas, their fracture toughness and thermal shock resistance are poor. Combining ceramics and metals [1-4], provides inherent advantages of these two kinds of materials, which has been pursued to meet the material requirements in many applications. The concept of functionally graded materials (FGMs) is now accepted worldwide and has been studied recently in many researches which are going to be summarized below. Due to these applications, thermo-mechanical behaviors of FGMs are becoming a major concern in recent research studies. For example, Burlayenko et al. [5] have used computational simulations to investigate thermal shock cracking by the virtual crack closure technique in a functionally graded plate. Sofiyev [6] with the use of shear deformation theory has investigated the thermo-elastic stability of freely supported functionally graded

[1] University of Tabriz, Iran, Islamic Republic Of, email: f_vakili@tabrizu.ac.ir
[2] University of Tabriz, Iran, Islamic Republic Of, email: nima.mahkam@yahoo.com
[3] University of Tabriz, Iran, Islamic Republic Of, email: arash.mafard@tabrizu.ac.ir

conical shells and the problem is reduced to a set of linear algebraic equations using the Galerkin's method. Naotake Noda [7] has been studied on thermal stresses and thermal stress intensity factors in the FGMs which are subjected to steady temperature fields or thermal shocks. Lately, Wang et al. [8] have studied the thermo elastic response of FG thin plates under thermal shocks in which the material properties are assumed to vary along the lengthwise direction with a power law. They linearized the governing equations by the layer method. Ghiasian et al. [9] perused on one dimensional non-linear thermal condition for FG beams via hybrid iterative central finite and Crank-Nicolson method in which thermo mechanical properties are temperature and position dependent. Ranjbar and Alibeigloo [10] studied analytical solution of an FG thick hollow sphere subjected to thermo-mechanical and time dependent loads using Differential Transform Method (DTM) and Laplace transform. Sheng-Hu Ding and Xing Li [11] have investigated the growth of insulated interface crack subjected to a steady-state heat flux. The problem has been solved under the assumption of plane strain and generalized plane stress using Fourier transform. Taheri et al. [12] have been employed the isogeometrical optimization method for functionally graded structures in thermo-mechanical processes. This optimization method has been applied to define volume fractions of the constituents. Kursa et al. [13] investigated on procedure for finding an optimal content in metal-ceramic for specific applications. Ashby [14] has provided a review paper on multi-objective optimization methods for choosing materials for specific problem in which compromises are required to strike a balance between gaining different goals in a problem. A feature which distinguishes FGMs and homogeneous structures is the thermo-mechanical properties which vary spatially on the medium. These non-homogeneous material properties affect transient temperature and thermal stress distributions, significantly. In addition, this spatial variation makes the problem analyze much more intricate, thus, no exact analytical solutions have been presented lately.

In this paper, a new method has been proposed based on the combining discretization and Fourier series to obtain the transient temperature and stress distribution on a FGM plate. For this purpose, a computer code has been developed; and, it is coupled with another code which has been designed to obtain the volume fraction distribution of the plate with the objective of optimum distribution for the strength ratio. Two different methods of optimization techniques have been employed with the use of control points in different locations. In this way, the optimization will be free of any imposed predefined material distribution functions. Cubic Hermite polynomials are used to interpolate the volume fraction values between control points. Also, to consider the manufacturing process, a constraint is introduced to limit the variation of the volume fraction in adjacent layers. Material distributions in this study have been

evaluated using both Mori-Tanaka and Fuzzy logic together with Hashin-Schtrikman lower bonds.

2. Problem Characteristics

An infinite FG plate is considered with the thickness of L and material properties of thermal conductivity k, density ρ, specific heat c, Young's modulus E and Coefficient of Thermal Expansion (CTE) α which all vary on the thickness of the plate in z direction depending on the volume fraction of materials (Figure 1). The governing equations are transient regarding the thermal shock effects. The initial value of the temperature in the plate is assumed to be uniform. The surfaces z=0 and z=L are suddenly exposed to constant temperatures of T_0 andT_L, respectively. Physical properties for two constituents of the FGM are given in Table 1.

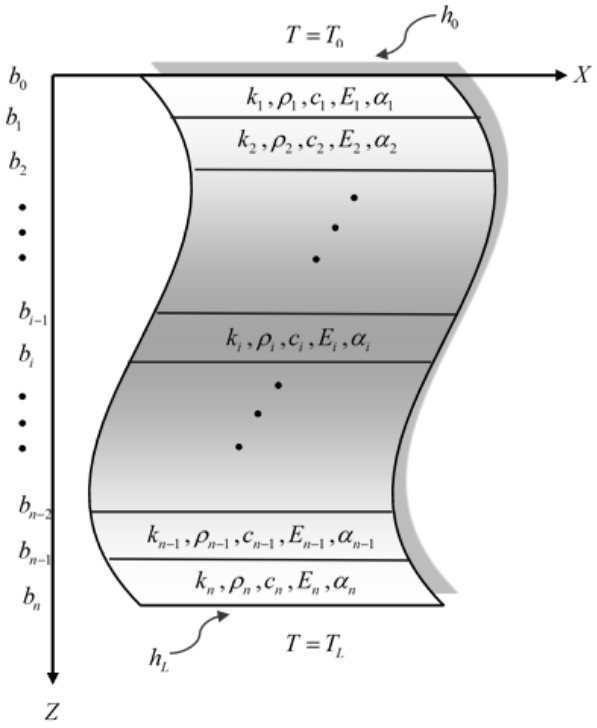

Figure 1. Functionally Graded plate

3. Material properties

It should be noticed that the FG structures are known as structures with continuous properties varying functionally in the medium. Two micromechanical formulations which are known to be used to estimate the equivalent properties of FGM are self-consistent [15] and Mori-Tanaka [16-19] methods. Another

method for evaluating the properties in FG structures is finite element method [20-21]. In this study the thermal conductivity, CTE and Young's Modulus are determined by Mori-Tanaka method in the region where volume fraction is less than 0.3 and greater than 0.7. Regarding the accuracy, Mori-Tanaka method is not valid in the region between 0.3 and 0.7 and thus, we take the advantage of Fuzzy logics to determine these properties in the region with the volume fraction between 0.3 and 0.7.

Table 1.Material properties of the Model

Material	Specific heat (J/kg.K)	Thermal conductivity (W/m.K)	Coefficient of thermal expansion (10^{-6} / $^{\circ}C$)	Density (kg/ m^3)	Young's modulus (GPa)
SiC	C_c =278	κ_c =2.09	α_c =10	ρ_c =3186.55	E_c = 442.44
Al 2024	C_m =897	κ_m =204	α_m =23	ρ_m =2973	E_m =78.05

Based on Mori-Tanaka method, Poisson's ratio and modulus of elasticity are introduced as equations (1) and (2):

$$v = \frac{3K - 2\mu}{6K + 2\mu} \tag{1}$$

$$E = \frac{9K\mu}{3K + \mu} \tag{2}$$

in which K and μ are the Bulk Modulus and shear Modulus expressed as equations (3) and (4):

$$K = \frac{V(K_2 - K_1)}{1 + (1 - \mathrm{V})\dfrac{K_2 - K_1}{K_1 + \dfrac{4}{3}\mu_1}} + K_1 \tag{3}$$

$$\mu = \frac{V(\mu_2 - \mu_1)}{1 + (1 - \mathrm{V})\dfrac{\mu_2 - \mu_1}{\mu_1 + f_1}} + \mu_1 \tag{4}$$

$$f_1 = \frac{\mu_1(9K_1 + 8\mu_1)}{6(K_1 + 2\mu_1)} \tag{5}$$

Conductivity *k* and thermal expansion α are obtained by equations (6) and (7):

$$\frac{k - k_1}{k_2 - k_1} = \frac{3k_1 V}{3k_1 + (1 - V)(k_2 - k_1)} \tag{6}$$

$$\frac{\alpha-\alpha_1}{\alpha_2-\alpha_1}=\frac{\frac{1}{K}-\frac{1}{K_1}}{\frac{1}{K_2}-\frac{1}{K_1}} \tag{7}$$

In all equations (3-7), the variables with subscript 1 are known as the base material and variables with subscript 2 are added ingredient.

In order to evaluate FG parametric values in equations (1-7) that are mentioned before, we use $\psi(\xi)$ which is described as equation (8);

$$\psi(\xi)=\begin{Bmatrix}\psi_1(\xi)\rightarrow 0<\xi<0.3\\ \psi_2(\xi)\rightarrow 0.7<\xi<1\end{Bmatrix} \tag{8}$$

In middle values $0.3<\xi<0.7$, we use fuzzy interpolation (Figure 2) to determine the value of $\psi(\xi)$ using $\psi_1(\xi)$ and $\psi_2(\xi)$. In addition, we need to define data functions with parameter ξ by equations (9) and (10):

$$\mu_1(\xi)=\frac{2(\xi-\frac{1}{2})^3}{\delta^3}-\frac{3(\xi-\frac{1}{2})}{2\delta}+\frac{1}{2} \tag{9}$$

$$\mu_2(\xi)=1-\mu_1(\xi) \tag{10}$$

in which δ =0.4 is the length of interpolation interval. For $0.3<\xi<0.7$, $\psi(\xi)$ is determined with equation (11);

$$\psi(\xi)=\text{Gravity}(\psi_1(\xi),\psi_2(\xi),\mu_1(\xi),\mu_2(\xi),\xi)\quad \text{in which } 0.3<\xi<0.7 \tag{11}$$

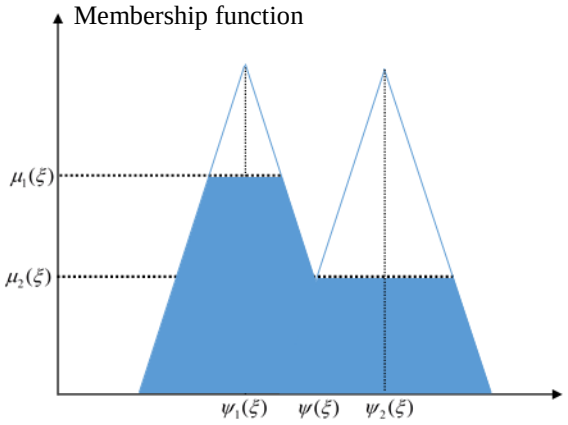

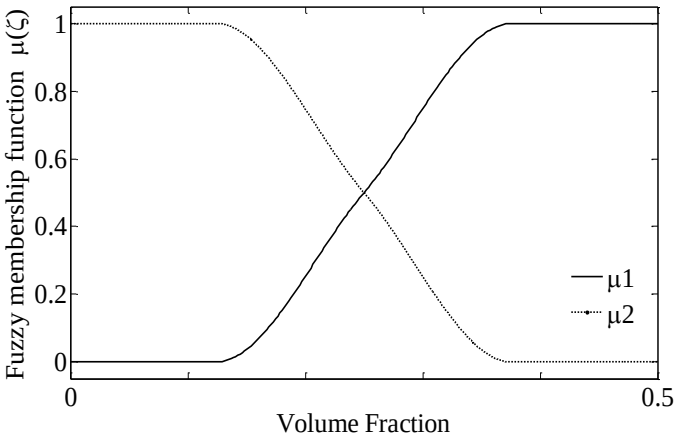

Figure 2. Data functions in Mori-Tanka method

Maximum allowable strength (S_y) for each layer along the FG plate is evaluated using Hashin-Schtrikman lower bond [22]:

$$S_y = \begin{cases} if\ \frac{2}{5}\sqrt{1+\frac{3V_1}{2}} < \frac{S_y^{(2)}}{S_y^{(1)}} \le 1\ \&\ V_1 < 1; \\ then\ \ \frac{5V_1}{3+2V_1} S_y^{(1)} + \frac{3V_2}{3+2V_1} S_y^{(2)} \sqrt{1+\frac{2V_1}{3}[1-(\frac{S_y^{(1)}}{S_y^{(2)}})^2]} \\ if\ \frac{S_y^{(2)}}{S_y^{(1)}} \le \frac{2}{5}\sqrt{1+\frac{3V_1}{2}}\ and\ V_1 < 1; then\ S_y^{(2)}\sqrt{1+\frac{3V_1}{2}} \\ if\quad V_1 = 1; then\ S_y^{(1)} \end{cases} \tag{12}$$

4. Material Distribution

In practice material distribution in FG plates is determined based on the manufacturing process. To achieve certain design characteristics, a favorite distribution is perused. Usually this distribution is defined based on optimization methods. However, using predefined material distribution functions impose a limitation for an optimum result. To overcome this shortcoming and to determine the optimum material distribution in the plate, one can define the volume fraction using control points. Between these control points, volume fraction can be interpolated. With dividing FG plate in to *n* layers and by selecting n+1 control points, the position of each control point is calculated by Eq. (13):

$$\varsigma_n = \varsigma_b + \frac{\varsigma_t - \varsigma_b}{N}(n-1),\ n = 1,...,N \tag{13}$$

in which ς_n, ς_b and ς_t are positions of n's, first and last control point on the plate. The volume fractions to the corresponding control points are λ_n, which the optimization variables are. After defining the values of λ_n in control points, the Hermite cubic interpolation functions are used as equations (14) to determine the volume fraction in other points:

$$\lambda(\varsigma)=\lambda_n H_1(\varsigma)+(\varsigma_{n+1}-\varsigma_n)S_n H_2(\varsigma)+\lambda_{n+1}H_3(\varsigma)+ (\varsigma_{n+1}-\varsigma_n)S_{n+1}H_4(\varsigma) \tag{14}$$

In equation (14), S_n is the distribution gradient percentage of the volume fraction in n's control point, the values of H are evaluated as:

$$H_1(\varsigma)=B_0\left(\frac{\varsigma-\varsigma_n}{\varsigma_{n+1}-\varsigma_n}\right)+B_1\left(\frac{\varsigma-\varsigma_n}{\varsigma_{n+1}-\varsigma_n}\right), H_2(\varsigma)=\frac{1}{3}B_1\left(\frac{\varsigma-\varsigma_n}{\varsigma_{n+1}-\varsigma_n}\right)$$
$$H_3(\varsigma)=B_2\left(\frac{\varsigma-\varsigma_n}{\varsigma_{n+1}-\varsigma_n}\right)+B_3\left(\frac{\varsigma-\varsigma_n}{\varsigma_{n+1}-\varsigma_n}\right), H_4(\varsigma)=-\frac{1}{3}B_2\left(\frac{\varsigma-\varsigma_n}{\varsigma_{n+1}-\varsigma_n}\right) \tag{15}$$

in which B_k is Bernstein polynomial:

$$B_k(t)=\binom{3}{k}t^k(1-t)^{(3-k)} \tag{16}$$

in which t stands for the Bernstein input variable. In Bernstein polynomial 3 and k are to be binomial coefficient.

Also values for the distribution gradient S_n are expressed by equation (17):

$$S_1=\frac{4\lambda_2-3\lambda_1-\lambda_3}{2(\varsigma_{n+1}-\varsigma_n)}$$
$$S_n=\frac{\lambda_{n+1}-\lambda_{n-1}}{2(\varsigma_{n+1}-\varsigma_n)},\quad n=2,3,\ldots,N \tag{17}$$
$$S_{N+1}=\frac{-4\lambda_N+3\lambda_{N+1}+\lambda_{N-1}}{2(\varsigma_{n+1}-\varsigma_n)}$$

5. Governing equations

5.1 Temperature distribution

As mentioned before the governing equations for conduction field must be transient as equation (18):

$$\frac{\partial\left[k(\xi)\partial \mathrm{T}/\partial\xi\right]}{\partial\xi}=\rho(\xi)\mathrm{c}(\xi)\frac{\partial T}{\partial\tau} \tag{18}$$

We take τ and T representing as non-dimensional time and temperature parameters described as $\tau=\kappa_m t/\mathrm{L}^2$ and $T=T^*/T_0$ where T^* and t are temperature and time respectively. It seems that there is no analytical solution for this equation, therefore to obtain a semi-analytical solution; the plate is divided to *n* layers in the *z* direction (Figure 1) in which all properties are constant. The heat transfer coefficients are assumed to be h_0 and h_L in edge parts of the plane. The transient heat conduction problem described in equation (18) can be described as equations (19-24) by taking the advantage of considering FG plate consist of n different layers:

$$k(\mathrm{i})\frac{\partial^2 T_i}{\partial\xi^2}=\rho(\mathrm{i})\,\mathrm{c}(\mathrm{i})\frac{\partial T_i}{\partial\tau} \tag{19}$$

$$T_i=25\ at\ \tau=0, i=1,2,...,n \tag{20}$$

$$k_0\frac{\partial T_0}{\partial\xi}+h_b(\mathrm{T}_0-\mathrm{T}_b(\tau))=0\ at\ \xi=b_0 \tag{21}$$

$$k_n\frac{\partial T_n}{\partial\xi}+h_L(\mathrm{T}_\mathrm{n}-\mathrm{T}_L(\tau))=0\ at\ \xi=b_n \tag{22}$$

$$T_i=T_{(\mathrm{i}+1)}\ at\ \xi=b_i, n=1,2,...\mathrm{n}-1 \tag{23}$$

$$k_i\frac{\partial T_i}{\partial\xi}=k_{(\mathrm{i}+1)}\frac{\partial T_{(i+1)}}{\partial\xi}\ at\ \xi=b_i, i=1,2,..,n-1 \tag{24}$$

In which ξ shows a non-dimensional parameter described as *z*/*L*. Parameter ξ can be evaluated considering the number of layers in region of b_0=0 and b_n=*L*/*L*=1, respectively. The solution for the equations (19-22) can be described as Fourier series shown in equations (25):

$$T_i(\xi,\tau)=(\sum_1^\infty(\varpi_{i,m}\sin(\omega_{i,m}\xi)+\nu_{i,m}\cos(\omega_{i,m}\xi))\exp(-\kappa(\mathrm{i})\omega_{i,m}\tau))+\Upsilon\xi+I \qquad b_i<\xi<b_{i+1} \tag{25}$$

In which $\omega_{i,m}$ (m=1, 2, 3…) denotes eigenvalues for each layer that can be calculated with the following condition.

$$\begin{pmatrix} a_{11} & \cdots & a_{1n} \\ \vdots & \ddots & \vdots \\ a_{m1} & \cdots & a_{mn} \end{pmatrix} = 0 \tag{26}$$

In which $a_{i,j}$ in the matrix are the values defined by the equations of boundary and continuous for the considered problem.

All values of the $\varpi_{i,m}$ and $\nu_{i,m}$ are nonzero and are evaluated with solving equation (27) :

$$[A]\{X\} = \{B\} \tag{27}$$

$$A = \begin{pmatrix} \text{Boundary Conditions Coeficients} \\ \text{Continuety Conditions Coeficients} \\ \text{Initial Condition Coeficients in Layer Boundaries} \\ \text{Initial Condition Coeficients in Sub-layers} \end{pmatrix} \tag{28}$$

$$B = \left(\text{The second side of the equations with all known values}\right)$$

It can be seen that the number of unknown variables in the above equations is more than the number of developed equations. To overcome this problem a number of new equations is produced by introducing new sub layers based on equation (20). The number of equations for each layer is the same as the number of unknown parameters $\varpi_{i,m}$, $\nu_{i,m}$ and $\omega_{i,m}$ (m=1, 2, 3…). The number of required subdivisions can be calculated using following steps:

- Determine the number of layers *(n)*
- Determine the satisfying number of eigenvalues (m) in equation (25)
- Determine the number of the developed equations to be solved
- Knowing that the number of all un-known parameters of equation (25) is equal to $2\times n\times m$,
  Then, the number of sub-layers can be obtained by subtracting the number of available equations from number of unknowns.

5.2 Stress distribution

Assuming an idealized thermal shock to happen, Erdogan and Wu [23] have determined the thermal stresses of a fully free FG plate as equation (29):

$$\sigma_{xx}(\xi,\tau) = \frac{E(\xi)}{1-\nu(\xi)}(\chi\xi + \vartheta - \alpha(\xi)(\mathrm{T}(\xi,\tau) - \mathrm{T}_0)) \tag{29}$$

in which T_0 is the initial temperature. The χ and ϑ are time dependent constants and are calculated by equations (30) and (31):

$$\int_0^L \sigma_{xx}(\xi)d\xi = 0 \tag{30}$$

$$\int_0^L \sigma_{xx}(\xi)\xi d\xi = 0 \tag{31}$$

Matrix method which is described in determining the temperature field, again is used in stress analyze to evaluate the parameters χ and ϑ. These two equations satisfy the boundary conditions applied to the free edges of the plate. By satisfying these two equations, all parametric values as χ and ϑ will be evaluated, resulting stress distribution in the plate in all point.

6. Optimization

In this work, Genetic Algorithm (GA) and Particle Swarm Optimization (PSO) methods are used to obtain the desired volume fraction distribution.

6.1 Genetic algorithm

Genetic algorithm is a method of optimization based on natural selection. This method optimizes the initial random population by a special selecting rule. The initial population is random, which includes the information about optimization variables (volume fraction in the control points). In the next step, objective function is evaluated and on this basis, the population is sorted. Then, half of the population members which are inappropriate are excluded. Among the remaining members, the algorithm chooses some data named as parents whom they will generate some new data. In this study, we have used the weighting method for selecting the parents. Corresponding probability for each rank, *n*, is evaluated with equation (32):

$$P_n = \sum_{i=1}^{n} \frac{\bar{N} - n + 1}{\sum_{n=1}^{\bar{N}} n} \tag{32}$$

In which $\bar{N}$ shows the number of remaining data which is equal to half of total population.

In the next step, after selecting the parents, a new generation is to be generated by applying continuous crossover operator so that each pair of parents generate two new members, while total population number is fixed. Next step is to evaluate the values of the objective function for new members. These steps are repeated till the solution is converged. To implement the constraints (equation (33)), Penalty function method (equations (34)) is used:

$$g(\mathrm{x}) \geq \mathrm{g}_0 \tag{33}$$

$$\hat{J} = J + \mathrm{P}\max\{0, [\mathrm{g}_0 - \mathrm{g}(\mathrm{x})]\} \tag{34}$$

in which g_0 is the threshold value of the constraint and $\hat{j}$ shows the objective function after applying the penalty function. The value of penalty coefficient P , is an extremely large number so that the constraint is satisfied.

6.2 Particle Swarm Optimization

Particle Swarm Optimization (PSO) method has been inspired from ordered movements of a flocks of fishes which are based on two main opinions: firstly, communication between different members of the population; and secondly, fitness of each member. As a base rule of the algorithm, all members have tendency to change their position and follow the best member with high fitness. Also, each member is obligated to memorize its own best position. This method works with numbers of data, named as particles. Best member of the population is chosen to be the leader which it makes other members to move toward it. As a result, considering the number of iteration, all of the population gathers around the leader, which may change in each iteration. This makes the algorithm to converge [24 - 26].

In PSO, each particle is an answer for the problem, and it is identified with a vector which the length of it is the number of designing parameters. Initial population is randomly produced with position of x_i^0 and speed v_i^0. After determining the leader, speed and position of the other particles are updated. Equations (35), (36) and (37) are the base equations of the algorithm;

$$v_i^{k+1} = \Omega v_i^k + \phi_1(\mathrm{g}^k - \mathrm{x}_i^k) + \phi_2(I_i^k - \mathrm{x}_i^k) \tag{35}$$

$$x_i^{k+1} = x_i^k + v_i^{k+1} \tag{36}$$

$$\phi_1 = r_1 a_1 \ , \ \phi_2 = r_2 a_2 \tag{37}$$

in which I_i^k and g^k are the values of the best answer for the particle i and best answer of the all population. Similarly, Ω, a_1 and a_2 are the coefficient of inertia and learning factors respectively, and r_1, r_2 are two random parameters in the range of zero and one. Larger coefficient of inertia results spreading the population on a plane without considering the best experience of each particle, on the other hand, small coefficient of inertia forbids each particle to alter and move on its own present values. It should be considered that the magnitude of these coefficients is less than one [25 - 27]. These values are considered to be constant

during the process based on equation (38) to simplify the method in contemporary projects [25]:

$$\Omega = \frac{1}{2\ln(2)} \approx 0.721 \tag{38}$$

Parameters a_1 and a_2 are the values which show how much each particle will alter based on the best personal and population experience (leader). The sum of all these values should be less than 4. Equations (39) and (40) show the suggested values given in references [24] and [25];

$$a_1 = a_2 = 2 \tag{39}$$

$$a_1 = a_2 = 0.5 + \ln(2) \approx 1.193 \tag{40}$$

After updating speed, each particle will move to its new position. If the updated position is the best position which the particle had experienced, the position will be collected as the best position till the next one occurs. Moreover, if the updated position is the best position among the all population it will be chosen as the leader. At the end, the position of the leader will be selected as the final answer for the algorithm.

6.3 Optimization formulation

To be able to evaluate the values of the optimum variables, the objective function and problem constraints are introduced as equations (41) and (42);

$$Obj = \min\left(\int (\frac{S_y}{\sigma} - SF) d\xi\right) \tag{41}$$

$$\left|\lambda_i - \lambda_{i-1}\right| < \delta\lambda \quad i = 1, 2, ..., n \tag{42}$$

In which σ is the value of stress in each layer and SF is to be ideal safety factor. The value of the objective function is to be minimized in order to have uniform factor of safety based on the maximum allowable strength in each layer. Also, equation (42) constraints the change of the volume fraction value in i^{th} layer comparing to the neighboring layers in the range of $\pm\delta\lambda$.

7. Validation

To validate the solution method, the temperature distribution along the z direction of a FG plate as a result of thermal shock in a harsh environment is obtained and compared with those reported by Wang et al. [28]. For this purpose or model verification, one-dimensional transient temperature distribution given by Wang for TiC and Ni has been used. Physical properties for TiC and Ni are given

in Table 2. Convection coefficients of the outer surfaces of the plate: h_0 and h_L are infinite in two sides, and the plate and boundary conditions are symmetric with respect to longitudinal axis. Two sides of the plate have been exposed to sudden temperature change in the very beginning of the heat conduction process. Results of both solution methods, those obtained with the proposed method and those reported by Wang [28], are shown in figure 3 and good agreement is observed.

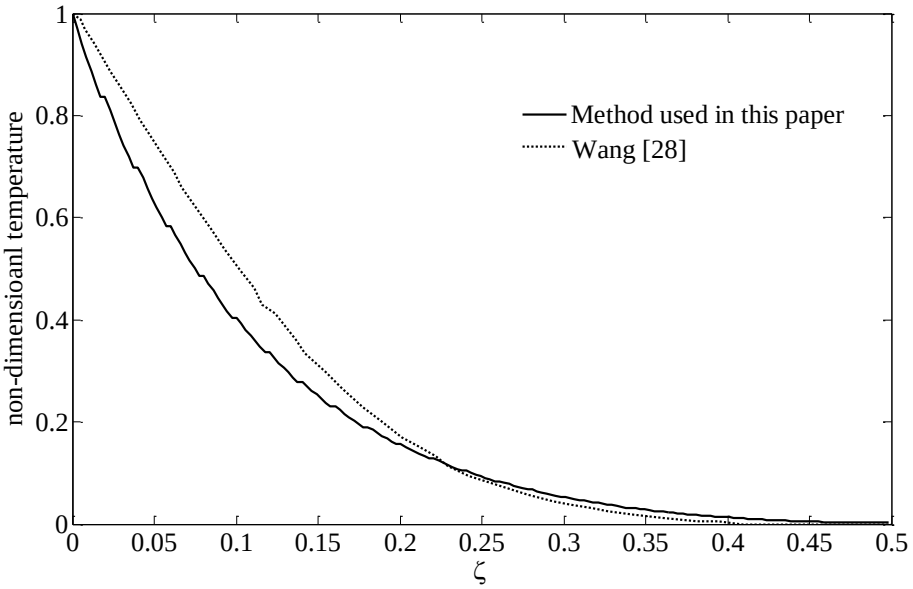

Figure 3. Results validation; Transient temperature distribution in a homogeneous layer.

Table 2.Material properties of the verified model

Material	Specific heat (J/kg.K)	Thermal conductivity (W/m.K)	Coefficient of thermal expansion ($10^{-6}/^{\circ}C$)	Density (g/cm^3)	Young's modulus (GPa)
TiC	C_c =134	κ_c =25.1	α_c =7.4	ρ_c =4.94	E_c = 320
Ni	C_m =439.5	κ_m =90.5	α_m =13.3	ρ_m =8.89	E_m =206

8. Results of optimum material distribution

Firstly, the temperature distribution for a FG Al2024/SiC plate, manufactured by Erdemir et al [29], is calculated using the proposed solution method. The results are obtained for a FG plate with h_0 and h_L equal to infinity and initial temperature of 25 centigrade degrees. Figure 4 and 5 show the convergence rate for GA and PSO respectively. These figures show that both solutions converge beyond 40 iterations the influence of provision lambda is noticeable in both two methods. Value of safety factor SF=S_y/σ obtained from these

optimization methods, and are shown in Figures 6 and 7 which are to be uniform in all over the plate as the optimization goal. It can be seen in these figures that PSO have resulted a better SF distribution for the plate than GA but with higher number of generations which as a sequence it needs more time to result a precise answer for the problem.

Maximum allowable stress for the pure aluminum and ceramic are assumed to be 112.3 MPa and 490.3 MPa, respectively. The distribution of the volume fraction along the z direction of the plate with non-dimensional parameter b_i for FG plate is illustrated in figures 8 and 10 for both methods. In Figures 9 and 11 the stress distribution on FG plate due to the thermal shock with $\delta\lambda = 0.45$ is presented by considering the time. As it can be seen from these figures PSO method provides more uniform stress distribution all over the plate rather than GA method.

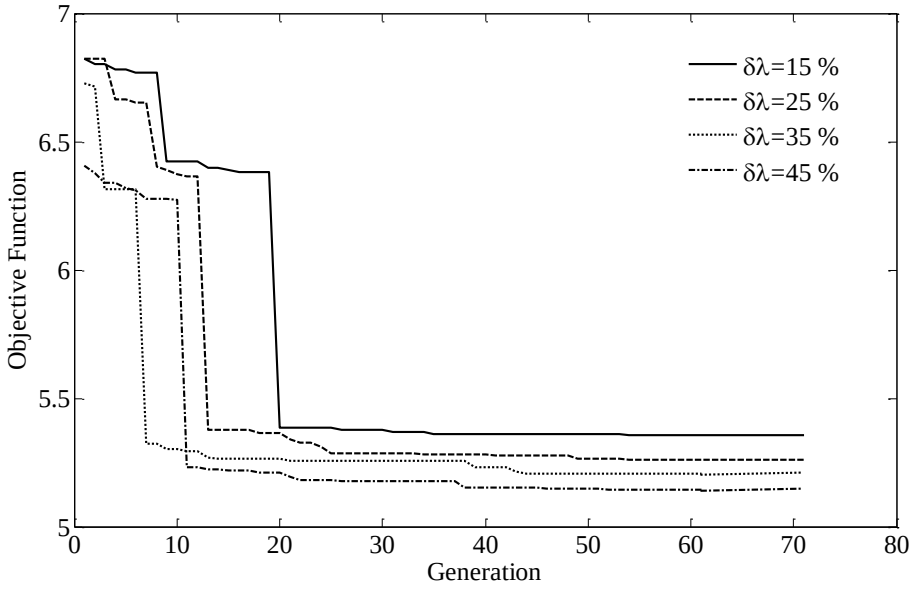

Figure 4. GA convergence rate in the FG plate with different range of lambda.

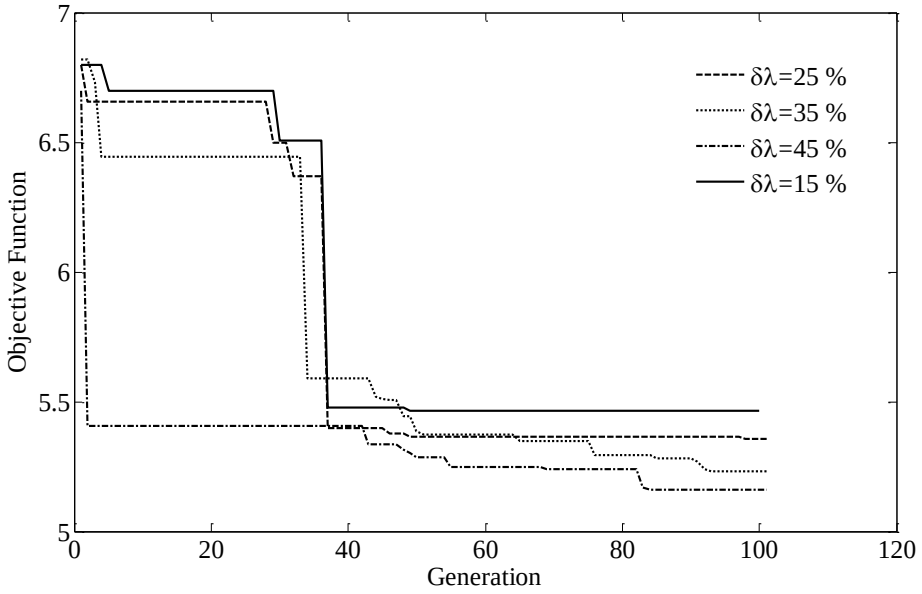

Figure 5. PSO convergence rate in the FG plate with different range of lambda.

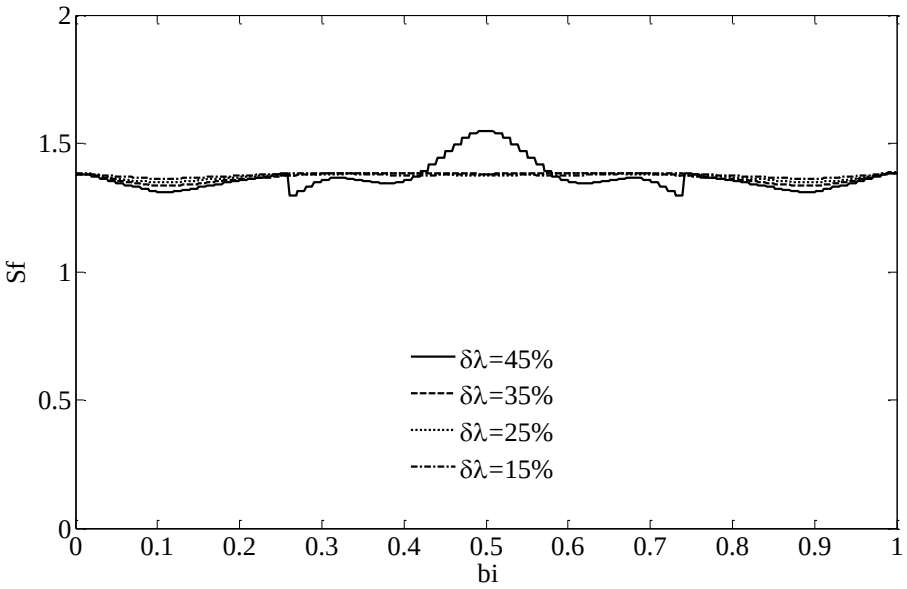

Figure 6. The best safety Factor ($\frac{S_y}{\sigma}$) distribution in all over the plate with different range of volume fraction provisions for GA.

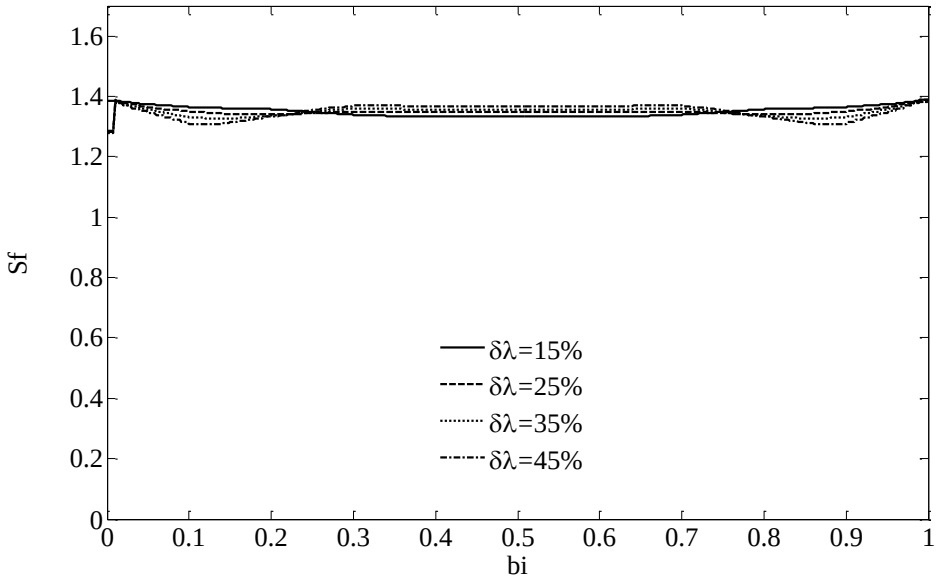

Figure 7. The best Safety Factor ($\frac{S_y}{\sigma}$) distribution in all over the plate with different range of volume fraction provisions for PSO.

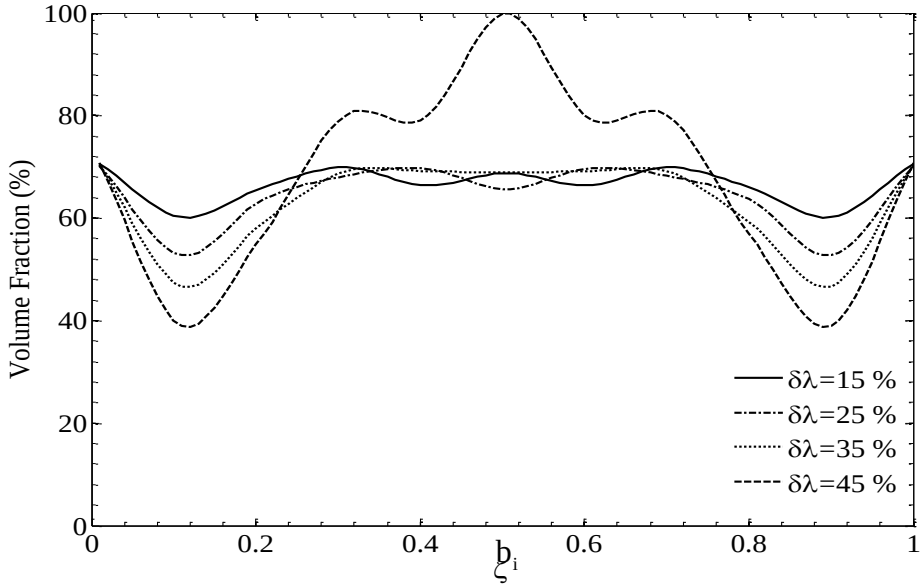

Figure 8. Volume fraction distribution along the z direction of FG plate with different range of lambda provision in genetic algorithm method.

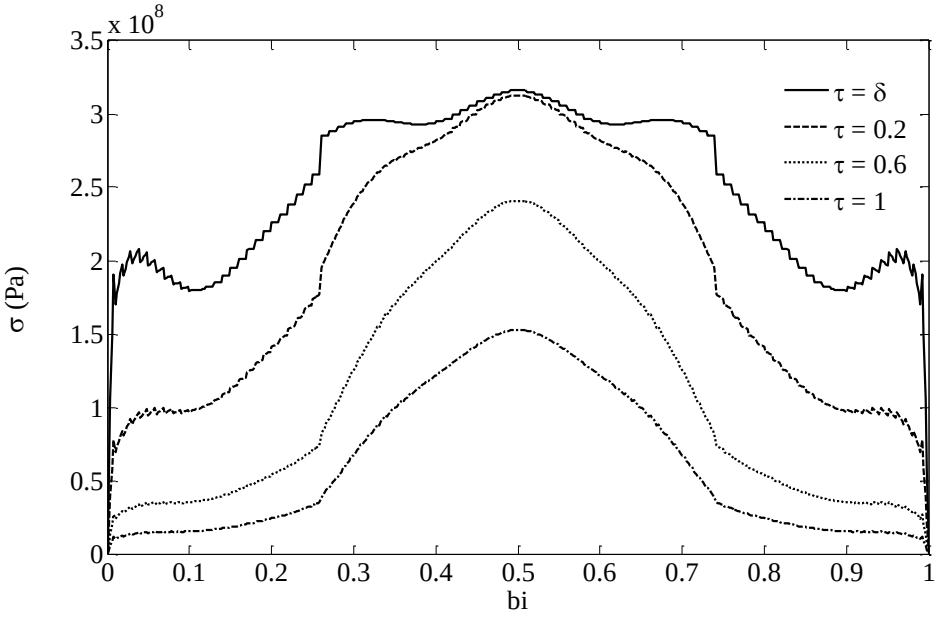

Figure 9. Stress distribution along the z direction of FG plate under thermal shock with volume fraction resulted with genetic algorithm method. δ Indicate small time pass after shock is exposed for lambda=45%.

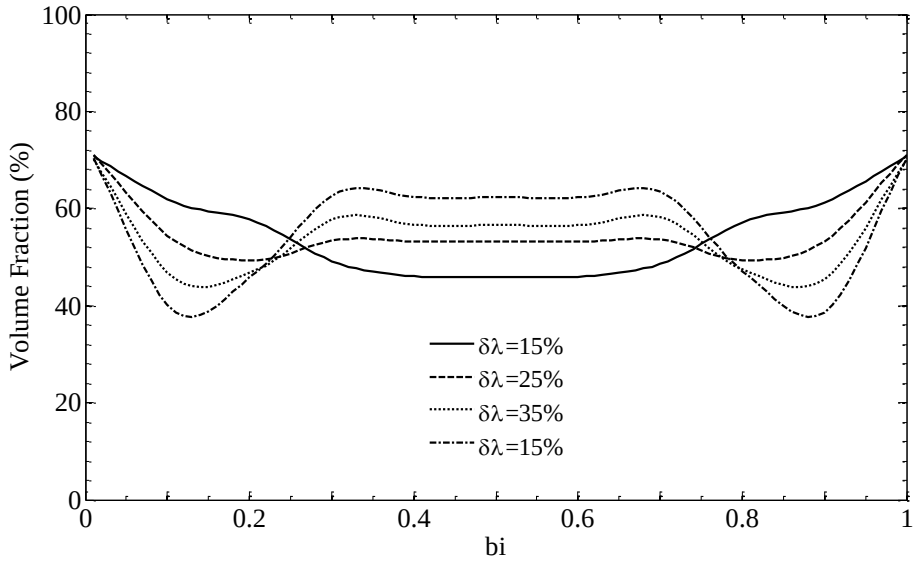

Figure 10. Volume fraction distribution along the z direction of FG plate with different range of lambda provision in PSO optimization method.

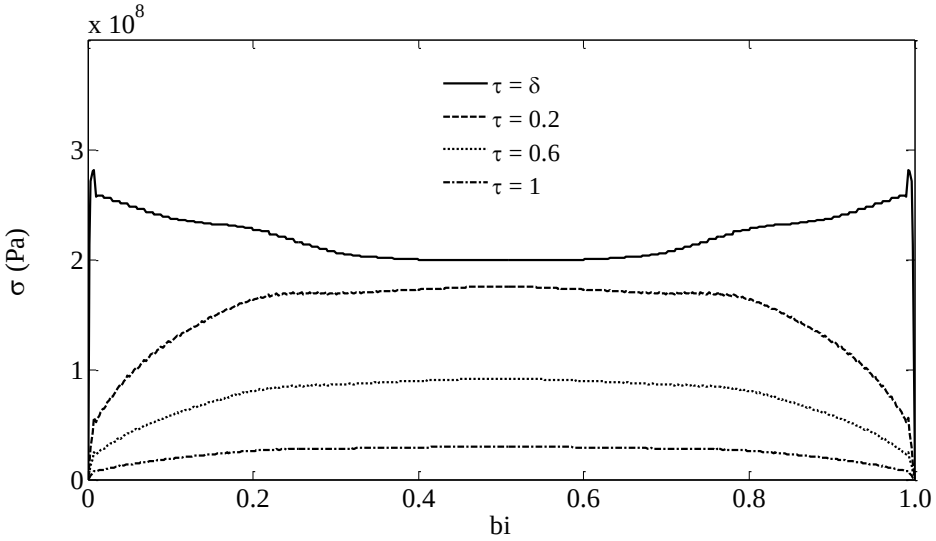

Figure 11. Stress distribution along the z direction of FG plate under thermal shock with volume fraction resulted with PSO method. δ Indicate small time pass after shock.

9. Conclusion

Transient thermal shock effect on a FG plate has been studied in this paper. Two different sides of the plate undergo a sudden temperature gradient. A computer code has been developed to obtain the temperature distribution along the z direction of the plate. The method is based on the combining discretization and Fourier series in space and time domain. Equivalent material properties have been evaluated with hybrid use of Mori-Tanaka and Fuzzy logic with considering Hashin-Schtrikman lower bonds. To evaluate the accuracy of the solution method, the results of this method are compared with the available data in the literature. A good agreement is observed.

This computer code is extended with the use of two different optimization methods: GA and PSO, which determine the FGM volume fraction distribution to provide optimum strength ratio along the plate. For this purpose, material distribution across the z direction of the plate is obtained in control points. Volume fraction distribution across the plate is interpolated using cubic Hermite polynomials which have been calculated using Bernstein polynomial. The results show the flexibility of the proposed method compared to other methods which use predefined volume fraction functions.

REFERENCES

[1*] Jha DK, Kant T, Singh RK*, A critical review of recent research on functionally graded plates. Composite Structures. 2013 Feb 28;96:833-49.

[2] *Miyamoto Y, Kaysser WA, Rabin BH, Kawasaki A*, Ford RG, editors. Functionally graded materials: design, processing and applications. Springer Science & Business Media; 2013 Nov 27. [3] Suresh S, Mortensen A. Functionally graded metals and metal-ceramic composites: Part 2 Thermomechanical behaviour. International Materials Reviews. 2013 Jul 18.

[4] *Shen HS*, Functionally graded materials: nonlinear analysis of plates and shells. CRC press; 2016 Apr 19.

[5] *Burlayenko VN, Altenbach H, Sadowski T, Dimitrova SD*, Computational simulations of thermal shock cracking by the virtual crack closure technique in a functionally graded plate. Computational Materials Science. 2016 Apr 15;116:11-21.

[6] *Sofiyev AH*, Thermoelastic stability of freely supported functionally graded conical shells within the shear deformation theory. Composite Structures. 2016 Sep 15;152:74-84.

[7] *Noda N*, Thermal stresses in functionally graded materials. Journal of Thermal Stresses. 1999 Jun 1;22(4-5):477-512.

[8] *Wang YZ, Liu D, Wang Q, Zhou JZ*, Asymptotic analysis of thermoelastic response in functionally graded thin plate subjected to a transient thermal shock. Composite Structures. 2016 Apr 1;139:233-42.

[9] *Ghiasian SE, Kiani Y, Eslami MR*, Non-linear rapid heating of FGM beams. International Journal of Non-Linear Mechanics. 2014 Dec 31;67:74-84.

[10] *Ranjbar J., Alibeigloo A.,* Response of functionally graded spherical shell to thermo-mechanical shock. Aerospace Science and Technology. 2016 Apr 30;51:61-9.

[11] *Ding SH, Li X.*, Thermoelastic analysis of nonhomogeneous structural materials with an interface crack under uniform heat flow. Applied Mathematics and Computation. 2015 Nov 15;271:22-33.

[12] *Taheri AH, Hassani B, Moghaddam NZ*., Thermo-elastic optimization of material distribution of functionally graded structures by an isogeometrical approach. International Journal of Solids and Structures. 2014 Jan 15;51(2):416-29.

[13] *Kursa M, Kowalczyk-Gajewska K, Petryk H.* , Multi-objective optimization of thermo-mechanical properties of metal–ceramic composites. Composites Part B: Engineering. 2014 Apr 30;60:586-96.

[14] *Ashby MF*., Multi-objective optimization in material design and selection. Acta materialia. 2000 Jan 1;48(1):359-69.

[15] *T. Mori, K. Tanaka*, Average stress in matrix and average elastic energy of materials with misfitting inclusions, Acta Metallurgica, **Vol. 21**, No. 5, pp. 571-574, 1973.

[16] T. Chen, G. J. Dvorak, Y. Benveniste, Mori-Tanaka estimates of the overall elastic moduli of certain composite materials, ASME Transactions Series E Journal of Applied Mechanics, **Vol. 59**, pp. 539-546, 1992.

[17] *Zuiker J, Dvorak G.*, The effective properties of functionally graded composites—I. Extension of the mori-tanaka method to linearly varying fields. Composites Engineering. 1994 Jan 1;4(1):19-35.

[18] *Benveniste Y.*, Mori-Tanaka estimates of the overall elastic moduli of certain composite materials. Journal of applied mechanics. 1992 Sep;59:539.

[19] *S. S. Vel*, Exact elasticity solution for the vibration of functionally graded anisotropic cylindrical shells, Composite Structures, **Vol. 92**, No. 11, pp. 2712-2727, 2010.

[20] *J. Guedes, N. Kikuchi*, Preprocessing and postprocessing for materials based on the homogenization method with adaptive finite element methods, Computer Methods in Applied Mechanics and Engineering, **Vol. 83**, No. 2, pp. 143-198, 1990.
[21] *J. Čadek, H. Oikawa, V. Šustek*, Threshold creep behaviour of discontinuous aluminium and aluminium alloy matrix composites: An overview, Materials Science and Engineering: A, **Vol. 190**, No. 1, pp. 9-23, 1995.
[22] *Goupee AJ, Vel SS*., Multi-objective optimization of functionally graded materials with temperature-dependent material properties. Materials & design. 2007 Dec 31;28(6):1861-79.
[23] *Erdogan F, Wu BH*., Crack problems in FGM layers under thermal stresses. Journal of Thermal stresses. 1996 Apr 1;19(3):237-65.
[24] *Haupt RL, Haupt SE*., Practical genetic algorithms. John Wiley & Sons; 2004 Jul 30.
[25] *Panigrahi BK, Shi Y, Lim MH*, editors. Handbook of swarm intelligence: concepts, principles and applications. Springer Science & Business Media; 2011 Feb 4.
[26] Clerc M. Particle swarm optimization. John Wiley & Sons; 2010 Jan 5.
[27] *Perez RE, Behdinan K.*, Particle swarm approach for structural design optimization. Computers & Structures. 2007 Oct 31;85(19):1579-88.
[28] *Wang BL, Mai YW, Zhang XH*., Functionally graded materials under severe thermal environments. Journal of the American Ceramic Society. 2005 Mar 1;88(3):683-90.
[29] *Erdemir F, Canakci A, Varol T.*, Microstructural characterization and mechanical properties of functionally graded Al2024/SiC composites prepared by powder metallurgy techniques. Transactions of Nonferrous Metals Society of China. 2015 Nov 1;25(11):3569-77.